Provided for non-commercial research and education use.
Not for reproduction, distribution or commercial use.



This article appeared in a journal published by Elsevier. The attached copy is furnished to the author for internal non-commercial research and education use, including for instruction at the authors institution and sharing with colleagues.

Other uses, including reproduction and distribution, or selling or licensing copies, or posting to personal, institutional or third party websites are prohibited.

In most cases authors are permitted to post their version of the article (e.g. in Word or Tex form) to their personal website or institutional repository. Authors requiring further information regarding Elsevier's archiving and manuscript policies are encouraged to visit:

http://www.elsevier.com/copyright

Author's personal copy

Biochimica et Biophysica Acta 1787 (2009) 1254–1265

Contents lists available at ScienceDirect

Biochimica et Biophysica Acta

journal homepage: www.elsevier.com/locate/bbabio

Preferential pathways for light-trapping involving β-ligated chlorophylls

Teodor Silviu Balaban [a,b,c,*], Paula Braun [d], Christof Hättig [a,e], Arnim Hellweg [a,e,f], Jan Kern [g], Wolfram Saenger [h], Athina Zouni [g]

[a] Karlsruhe Institute of Technology, Forschungszentrum Karlsruhe, Institute for Nanotechnology, Postfach 3640, D-76021 Karlsruhe, Germany
[b] Center for Functional Nanostructures, Universität Karlsruhe (TH), Germany
[c] Université "Paul Cézanne" Aix-Marseille III, ISM2, UMR 6263 Chirosciences, Ave. Escadrille Normandie Niemen, St. Jérôme, F-13397 Marseille, CEDEX 20, France
[d] Ludwig-Maximilians-Universität München, Department Biologie I – Botanik, Menzinger Straβe 67, D-80638 München, Germany
[e] Ruhr-Universität Bochum, Lehrstuhl für Theoretische Chemie, Universitätsstraβe 150, D-44801 Bochum, Germany
[f] COSMOlogic GmbH&Co.KG, Burscheider Str. 515, D-51381 Leverkusen, Germany
[g] Technische Universität Berlin, Institut für Chemie, Max-Volmer Laboratorium für Biophysikalische Chemie, Straβe des 17. Juni 135, D-10623 Berlin, Germany
[h] Freie Universität Berlin, Institut für Chemie und Biochemie/Kristallographie, Takustaβe 6, D-14195 Berlin, Germany

ARTICLE INFO

Article history:
Received 16 March 2009
Received in revised form 18 May 2009
Accepted 20 May 2009
Available online 27 May 2009

Keywords:
Crystal structure
Photosystem I
Photosystem II
Diastereotopicity
Chlorophyll complex
ab initio calculation

ABSTRACT

The magnesium atom of chlorophylls (Chls) is always five- or six-coordinated within chlorophyll–protein complexes which are the main light-harvesting systems of plants, algae and most photosynthetic bacteria. Due to the presence of stereocenters and the axial ligation of magnesium the two faces of Chls are diastereotopic. It has been previously recognized that the α-configuration having the magnesium ligand on the opposite face of the 17-propionic acid moiety is more frequently encountered and is more stable than the more seldom β-configuration that has the magnesium ligand on the same face [T.S. Balaban, P. Fromme, A.R. Holzwarth, N. Krauβ, V.I. Prokhorenko, Relevance of the diastereotopic ligation of magnesium atoms in chlorophylls in Photosystem I, Biochim. Biophys. Acta (Bioenergetics), 1556 (2002) 197–207; T. Oba, H. Tamiaki, Which side of the π-macrocycle plane of (bacterio)chlorophylls is favored for binding of the fifth ligand? Photosynth. Res. 74 (2002) 1–10]. In photosystem I only 14 Chls out of a total of 96 are in a β-configuration and these occupy preferential positions around the reaction center. We have now analyzed the α/β dichotomy in the homodimeric photosystem II based on the 2.9 Å resolution crystal structure [A. Guskov, J. Kern, A. Gabdulkhakov, M. Broser, A. Zouni, W. Saenger, Cyanobacterial photosystem II at 2.9 Å resolution: role of quinones, lipids, channels and chloride, Nature Struct. Mol. Biol. 16 (2009) 334–342] and find that out of 35 Chls in each monomer only 9 are definitively in the β-configuration, while 4 are uncertain. *Ab initio* calculations using the approximate coupled-cluster singles-and-doubles model CC2 [O. Christiansen, H. Koch, P. Jørgensen, The second-order approximate coupled cluster singles and doubles model CC2, Chem. Phys. Lett. 243 (1995) 409–418] now correctly predict the absorption spectra of Chls *a* and *b* and conclusively show for histidine, which is the most frequent axial ligand of magnesium in chlorophyll–protein complexes, that only slight differences (<4 nm) are encountered between the α- and β-configurations. Significant red shifts (up to 50 nm) can, however, be encountered in excitonically coupled β–β-Chl dimers. Surprisingly, in both photosystems I and II very similar "special" β–β dimers are encountered at practically the same distances from P700 and P680, respectively. In purple bacteria LH2, the B850 ring is composed exclusively of such tightly coupled β-bacteriochlorophylls *a*. A statistical analysis of the close contacts with the protein matrix (<5 Å) shows significant differences between the α- and β-configurations and the subunit providing the axial magnesium ligand. The present study allows us to conclude that the excitation energy transfer in light-harvesting systems, from a peripheral antenna towards the reaction center, may follow preferential pathways due to structural reasons involving β-ligated Chls.

© 2009 Elsevier B.V. All rights reserved.

1. Introduction

The vast majority of chlorophylls (Chls), which are ubiquitous natural pigments, are primarily responsible for light-harvesting in photosynthetic organisms. Efficient photon capture of solar radiation is assured by large assemblies of Chl molecules either within chlorophyll–protein complexes (CPCs) or within self-assembled nanoarchitectures [1–3]. *Energy transfer* steps assure that eventually the radiation is

Abbreviations: PS, photosystem; RC, reaction center; CPC, chlorophyll–protein complex; Chl, chlorophyll; LHC, light-harvesting complex; CC2, coupled-cluster singles-and-doubles

* Corresponding author. Karlsruhe Institute of Technology, Forschungszentrum Karlsruhe, Institute for Nanotechnology, Postfach 3640, D-76021 Karlsruhe, Germany. Fax: +49 7247 82 9030.
E-mail address: silviu.balaban@int.fzk.de (T.S. Balaban).

0005-2728/$ – see front matter © 2009 Elsevier B.V. All rights reserved.
doi:10.1016/j.bbabio.2009.05.010

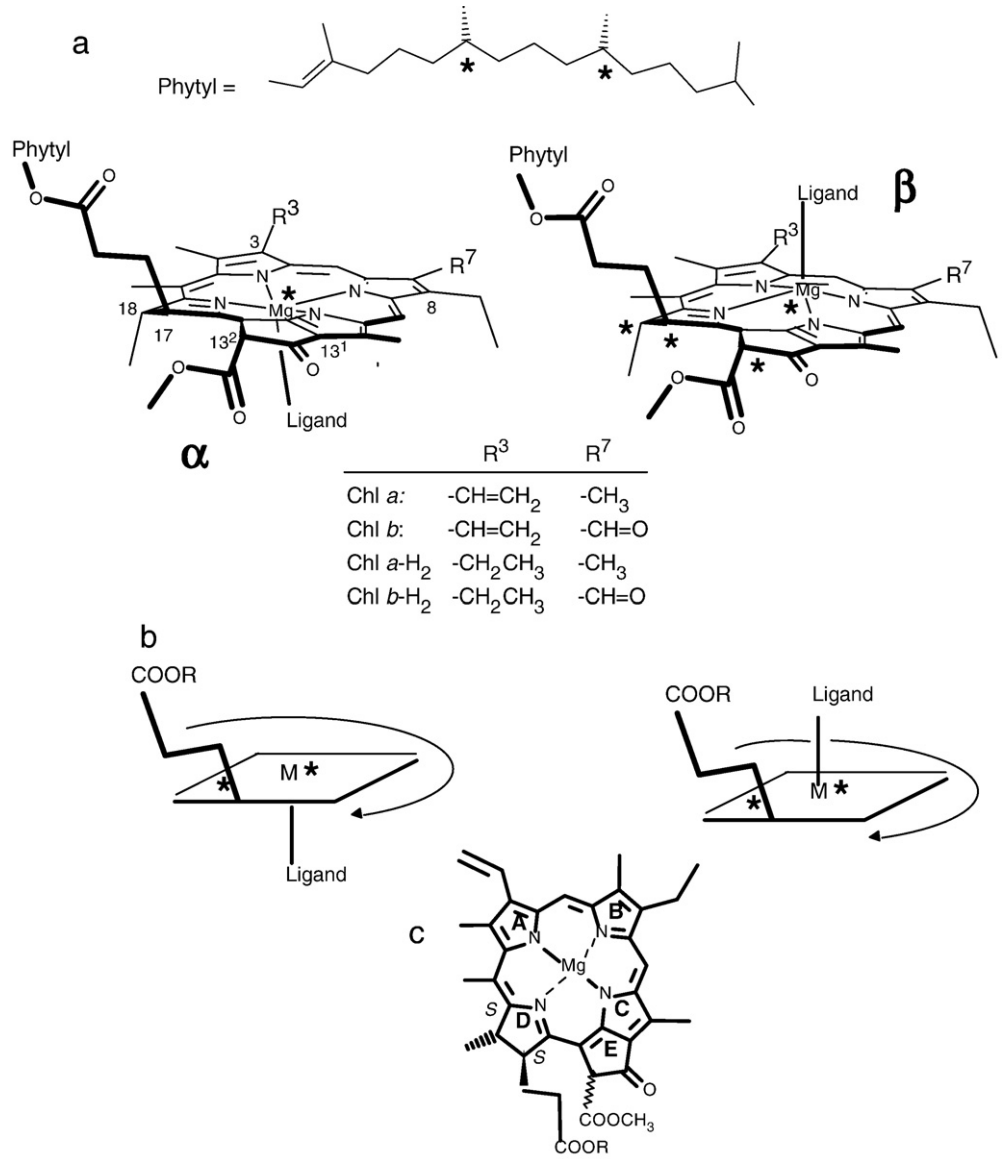
Author's personal copy

trapped within reaction centers (RC) formed from a few specialized Chls capable of charge separation and directing subsequent *electron transfer* steps [4]. The RC-CPC is unique for converting light into biochemical energy. The bacterial RC [5] and the plant photosystems PSI [6–8] and PSII [9–13] all present strikingly similar architectures of the specialized RC-Chls, indicating that organisms having less efficient charge separation machines have not survived the evolutionary pressure. In stark contrast is the large variety of light-harvesting (LH) systems. These comprise the elliptical purple bacterial LH1 [14,15] and circular LH2 [16–18] complexes, the phycobilisomes of cyanobacteria and red algae [19] or even the chlorosomes of green photosynthetic bacteria [20–25], all of which are very different from the plant LH complexes, LHCI being associated with PSI [8] and LHCII mainly with PSII [26–28].

An important yet unanswered question is how come light-harvesting is so efficient across a variety of species and habitats? Are there preferential pathways engineered by CPCs for funneling the energy captured by a peripheral antenna to the RC, or is the CPC just an amorphous conglomeration of pigments with an increased photon capture cross section, so that practically any photon captured will have its energy eventually trapped by an energetic sink?

We were fascinated by CPC architectures which have only very recently became known to atomic resolution [1–19,29,30]. Currently we are trying to understand and further mimic light-harvesting with artificial systems [23,24]. We noted in several CPCs that when the protein ligand coordinates the magnesium atom from the opposite side of the 17-propionyl acid substituent which is esterified by a long chain alcohol, such as phytol in the case of Chls, this leads to more stable structures which are encountered more frequently. This ligation is denoted by α. The alternative β-coordination is uncommon but preferentially occupies positions around the RC in PSI [31].

These stereochemical details of magnesium ligation are pictured in Fig. 1 for Chl *a* or *b* molecules. Chls have several carbon atoms with four different substituents that are stereocenters (indicated by asterisks in Fig. 1) and thus render Chls intrinsically chiral tetrapyrroles. Recently,



	R^3	R^7
Chl *a*:	$-CH=CH_2$	$-CH_3$
Chl *b*:	$-CH=CH_2$	$-CH=O$
Chl *a*-H_2	$-CH_2CH_3$	$-CH_3$
Chl *b*-H_2	$-CH_2CH_3$	$-CH=O$

Fig. 1. α/β Nomenclature for describing the diastereotopic ligation of tetrapyrroles. a) Shown are Chl *a* and Chl *b* molecules with the IUPAC clockwise atom numbering (arrows in the cartoons in part b). In the dihydro-Chls, R^3 is an ethyl substituent. Asterisks denote chiral atoms. The α-configuration has the ligand below the chiral tetrapyrrolic plane (on the opposite side of the substituent at C17), while the β-configuration has the ligand above this plane. The central metal atom is thus an additional stereocenter. The β-configuration is given by a "left hand rule": if the fingers point clockwise, then the left thumb points upwards to the metal ligand. Analogously, the α-configuration is given by a "right hand rule". c) Typical text book formula of Chls *a* showing rings A–E of the chlorin tetrapyrrole. The stereochemistry at $C13^2$ in ring E is *R* in Chl *a* and *S* in the epimer Chl *a*'. Note that the magnesium atom in this representation is shown as four coordinate, lacking the fifth ligand. This coordination has never been encountered experimentally as in all crystal structures the magnesium atom in tetrapyrroles is five- or six-coordinate [47]). Figure adapted from reference [33].

Author's personal copy

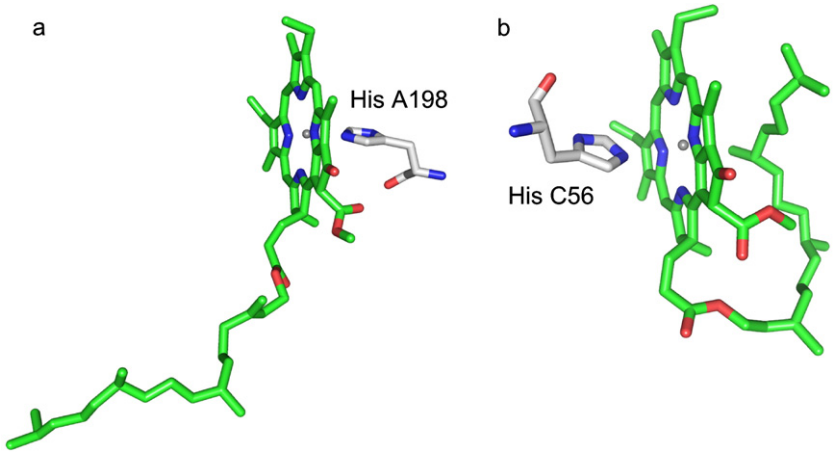


Fig. 2. Two Chl *a* molecules and the amino acids ligating the central Mg^{2+} as seen in the structural model of cyanobaterial PSII at 2.9 Å resolution [13]. a) Chl A362 (Chl P_{D1}), with its central Mg^{2+} being ligated from its α side by His A198 (subunit D1). b) Chl C483 (Chl 46), with its central Mg^{2+} being ligated from its β side by His C56 (subunit CP43). For all of the Chls *a* the phytyl chain can be fitted completely to the electron density in the new 2.9 Å resolution data [13], allowing the α/β assignment if the fifth ligand to the central Mg^{2+} is unambiguous. Carbon atoms are green, nitrogen blue, oxygen red and magnesium grey spheres. Carbon atoms of ligating His are shown in light grey. Figure was generated using PyMol and PDB entry 3bz1.

Balaban [31–33], Oba and Tamiaki [34–36] have pointed out that the central magnesium atom within the tetrapyrrolic macrocycle is coordinated by a fifth ligand in diastereotopic fashions, being thus a "metallic" additional stereocenter which leads to a dichotomy of Chls in natural and artificial systems [31–36]. As diastereomers have entirely different chemical and physical properties, it was highly probable that α-ligated Chls, which are also energetically more stable, have different absorption and fluorescence wavelengths or lifetimes and quantum yields than the "special" and more rarely encountered β-ligated Chls.

In earlier papers [31,32] we used the denomination "*anti*" for the α-ligation and "*syn*" for the β-ligation of the Mg atom. Independently, Oba and Tamiaki named these ligations "*back*" and "*front*"-face coordination, respectively [34,35] and this has unfortunately led to confusion and low acceptance of either proposed nomenclature. Presently, the α/β notation agrees with the IUPAC nomenclature rules for tetrapyrroles [33,36].

It was especially debated whether there is any biochemical relevance connected with the α/β-Chl-ligation. After analysing the interactions between the Chls and the protein matrix [37], it is now generally accepted that the preferential α ligation of Chls within CPCs is not a random phenomenon.

Based on the recent high resolution X-ray structure of the homodimeric PSII [13], we were in a unique position to accurately determine the α/β-configuration of the 35 Chls per monomer. Fig. 2 presents typical α- and β-Chls from PSII. We discovered very similarly positioned β-Chls as previously reported for PSI [31,32] which could thus function as the ultimate energy traps of the antenna pigments. With high level *ab initio* theoretical calculations we infer, for the first time, that the α- or β-histidine ligated Chl monomers do not differ significantly in their optical properties, but due to their "free face" interaction, a Chl···Chl dimer involving at least one β-ligated can be more tightly excitonically coupled giving rise to "red chlorophylls" which have been a much sought target in photosynthesis research. Alternatively, the interaction with the protein matrix can lead to different site energies for β-ligated Chls. Understanding the details of natural photosynthesis is essential for replicating in artificial, man-made devices for light-harvesting and subsequent photoinduced charge separation in order to efficiently convert solar radiation into other forms of energy or fuels.

2. Results and discussion

2.1. Ab initio calculations on α- and β-histidine ligated chlorophylls

In order to address whether the α- *versus* β-ligation of Chls has a pronounced effect on the photophysical properties, high level *ab initio* calculations were performed for histidine ligated Chl *a* and Chl *b* with the approximate coupled-cluster singles-and-doubles method CC2 [38] and the perturbative doubles correction to the configuration-interaction singles (or coupled-cluster singles) method CIS(D) [39]. Additionally the dihydro-Chls where the 3-vinyl group is reduced to an ethyl group (see Fig. 1) have been calculated as model compounds for understanding the reliability of our computational methods. These calculations became possible by a recently developed parallel implementation of the MP2, CIS(D) and CC2 methods [40,41], which employs a resolution-of-the-identity approximation to enhance the integral evaluations. All calculations have been performed with the TURBOMOLE programme package [42] and used for the resolution of the identity of accurately optimized auxiliary basis sets [43].

For the quantum chemical calculations the phytyl chain has been replaced by a methyl group. However, since the excitations of the phytyl ester group appear only below 250 nm, this should not affect the calculated spectra in the visible region above 430 nm. For all structures the ground state equilibrium geometries have been optimized at the DFT/B3LYP/TZVP level for several conformers. For the final calculation of the spectra, the energetically lowest conformers have been selected based on MP2/cc-pVDZ energies. To simulate the UV/Vis spectra the excitation energies for the lowest 30 transitions have been calculated at the CC2/cc-pVDZ level and the corresponding oscillator strengths at the coupled-cluster singles CCS/cc-pVDZ level by using the results of the CIS(D) perturbative corrections for assignment.

Table 1 presents the vertical excitation energies while Fig. 3 summarizes the results for Chl *a* and Chl *b* using the CC2 method. As spectra for dihydrochlorophylls are presently lacking, the stick diagrams of only the calculated spectra are not so informative, and these are not shown. For the first time it was now possible to more accurately predict the electronic ground state absorption spectra of Chls than with previous approaches [44,45]. These earlier time-dependent density functional theory (TD-DFT) calculations suffer from inherent problems and artificial bands in case of long range correlation effects and charge-transfer excitations. A more recent study on porphyrin free base and Chl *a* has shown that a Coulomb-attenuated exchange-correlated functional (CAM-B3LYP) can overcome these problems and accurately predicts charge-transfer spectra [46]. However, all these previous approaches have completely neglected the fifth ligand on the magnesium atom. It is unfortunate that chemistry and biochemistry textbooks still present (B)Chls with an unsaturated tetracoordinated magnesium atom which has never been encountered experimentally. All crystal structures of CPCs and chlorophyllides show that in addition to the tetrapyrrole, a fifth, or even a sixth ligand completes the coordination sphere of magnesium

Author's personal copy

Table 1
The vertical excitation energies of the different chromophores (see text for the acronyms)[a].

CC2		CIS(D)		*f*	CC2		CIS(D)		*f*
cm^{-1}	nm	cm^{-1}	nm		cm^{-1}	nm	cm^{-1}	nm	
α-Chl *a*					β-Chl *a*				
17,845.125	560.38	17,409.61	574.40	0.024	17,777.243	562.52	17,525.56	570.60	0.022
18,732.023	533.85	18,337.17	545.34	0.001	18,710.151	534.47	18,156.69	550.76	0.003
25,683.583	389.35	25,261.85	395.85	0.516	25,772.121	388.02	25,228.41	396.38	0.710
26,624.252	375.60	26,316.70	379.99	0.465	26,606.810	375.84	26,262.52	380.77	0.477
27,629.599	361.93	28,011.52	357.00	0.013	27,539.610	363.11	27,783.07	359.93	0.021
27,895.966	358.47	29,684.57	336.88	0.181	28,140.442	355.36	29,595.47	337.89	0.172
28,609.332	349.54	29,772.73	335.88	0.357	28,645.425	349.10	30,171.37	331.44	0.328
30,437.154	328.55	31,658.91	315.87	0.176	30,434.123	328.58	31,575.78	316.70	0.179
31,991.677	312.58	31,754.11	314.92	0.002	32,196.797	310.59	31,669.16	315.76	0.001
32,180.969	310.74	31,896.87	313.51	0.088	32,367.963	308.95	32,097.32	311.55	0.033
32,879.987	304.14	32,405.62	308.59	0.036	33,124.859	301.89	32,337.86	309.24	0.128
33,167.063	301.50	35,090.13	284.98	0.006	33,339.486	299.94	36,074.07	277.21	0.022
α-Chl *b*					β-Chl *b*				
17,810.642	561.46	17,217.04	580.82	0.032	17,793.404	562.01	17,256.22	579.50	0.035
18,481.012	541.10	18,193.64	549.64	0.028	18,454.716	541.87	18,145.98	551.09	0.027
23,698.161	421.97	23,599.97	423.73	0.762	23,591.010	423.89	23,519.56	425.18	0.915
25,166.392	397.36	23,611.33	423.53	0.410	25,086.318	398.62	24,321.16	411.16	0.283
27,901.986	358.40	29,182.38	342.67	0.330	27,963.232	357.61	28,881.01	346.25	0.409
28,651.664	349.02	30,326.63	329.74	0.002	28,535.056	350.45	30,331.29	329.69	0.005
29,755.671	336.07	30,494.70	327.93	0.176	29,749.032	336.15	30,963.64	322.96	0.001
29,928.094	334.13	31,517.71	317.28	0.003	30,034.244	332.95	31,068.86	321.87	0.176
31,377.615	318.70	31,646.00	316.00	0.001	31,549.928	316.96	31,692.42	315.53	0.001
31,952.687	312.96	32,194.47	310.61	0.101	32,247.158	310.10	32,687.68	305.93	0.035
32,530.898	307.40	33,245.65	300.79	0.049	32,944.010	303.55	32,773.34	305.13	0.076
32,783.639	305.03	34,098.69	293.27	0.337	33,139.440	301.76	34,054.13	293.65	0.342
α-Chl *a*	dihydro				β-Chl *a*	dihydro			
18,030.277	554.62	17,309.13	577.73	0.018	17,980.210	556.17	17,432.53	573.64	0.016
18,969.848	527.15	18,565.35	538.64	0.001	18,972.990	527.07	18,412.39	543.11	0.005
25,917.097	385.85	25,569.83	391.09	0.675	26,016.578	384.37	25,608.39	390.50	0.844
26,967.503	370.82	27,708.14	360.90	0.228	26,999.680	370.37	27,252.59	366.94	0.310
27,954.041	357.73	28,653.54	349.00	0.041	27,880.099	358.68	28,823.79	346.94	0.059
28,586.128	349.82	29,163.25	342.90	0.332	28,702.576	348.40	29,651.57	337.25	0.259
28,851.692	346.60	29,949.46	333.90	0.206	29,035.014	344.41	29,947.09	333.92	0.203
31,064.874	321.91	31,978.09	312.71	0.002	31,154.234	320.98	31,923.67	313.25	0.002
32,371.845	308.91	32,136.57	311.17	0.087	32,581.146	306.93	32,588.09	306.86	0.129
32,545.011	307.27	32,749.76	305.35	0.122	32,764.050	305.21	32,613.22	306.62	0.121
33,400.084	299.40	35,248.6	283.70	0.073	33,610.080	297.53	35,331.54	283.03	0.049
33,494.238	298.56	36,212.17	276.15	0.034	33,806.566	295.80	35,465.10	281.97	0.078
α-Chl *b*	dihydro				β-Chl *b*	dihydro			
17,985.477	556.00	17,370.62	575.68	0.023	17,486.325	571.88	17,358.43	576.09	0.042
18,650.890	536.17	18,345.06	545.11	0.029	18,270.278	547.34	17,922.62	557.95	0.041
23,997.229	416.71	23,733.14	421.35	0.443	23,286.644	429.43	22,601.57	442.45	0.405
25,410.163	393.54	23,960.44	417.35	0.841	24,637.154	405.89	22,707.65	440.38	0.929
28,674.396	348.74	30,260.45	330.46	0.001	29,224.358	342.18	30,175.04	331.40	0.085
28,976.335	345.11	30,336.21	329.64	0.122	30,117.127	332.04	30,768.50	325.01	0.106
29,838.577	335.14	30,455.39	328.35	0.200	31,791.887	314.55	30,790.60	324.77	0.015
30,021.759	333.09	31,623.03	316.23	0.002	32,009.491	312.41	31,749.69	314.96	0.288
31,770.278	314.76	31,705.55	315.40	0.001	32,034.397	312.16	32,439.44	308.27	0.002
32,501.080	307.68	32,366.46	308.96	0.118	32,550.579	307.21	32,827.19	304.63	0.001
32,919.223	303.77	34,278.25	291.73	0.148	33,000.441	303.03	32,884.69	304.09	0.108
33,111.353	302.01	35,123.82	284.71	0.167	33,270.736	300.56	35,047.52	285.33	0.240

[a] The oscillator strength (*f*) is calculated with CCS in mixed gauge.

[47]. Only very recently the role of the axial ligands for the structure and function of Chls has been considered [48] with respect to the assembly of LH complexes [49].

In our case an arbitrary scaling factor was used in order to match the experimental spectrum accounting for solvent effects, a remaining correlation and basis set error. Especially the so-called "chlorophyll green gap" between 450 and 600 nm, where no transitions are encountered is satisfactorily reproduced by our calculations. Also well reproduced is the more red-shifted Soret band and the more blue-shifted Q_y band of Chl *b* in comparison to Chl *a*. Only for the Q bands the intensities are predicted too low relatively to those of the Soret band. The Q bands, however, gain much intensity through vibronic coupling which has not been included in our quantum chemical calculations.

Another important result from the present *ab initio* calculations is evident from Fig. 3. It shows that there are no significant differences in the optical properties of the isolated α- or β-histidine ligated monomers in the gas phase. The only difference is that for Chl *b* a shoulder to the blue of the Soret band at ~430 nm is more intense for the α-ligation. For the first time, it is now possible to state that if different photophysical properties are due to the diastereotopic ligation of the Chls, these must be induced by strong interactions either within dimers/small aggregates, or with the apoprotein.

The effect of the double bond of the 3-vinyl substituent (R^3 in Fig. 1 a) is of particular interest because, when in full conjugation with the tetrapyrrole, it can lead to a significant bathochromic shift (more than 10 nm) in comparison with a 3-ethyl group. This allows for fine tuning

Author's personal copy

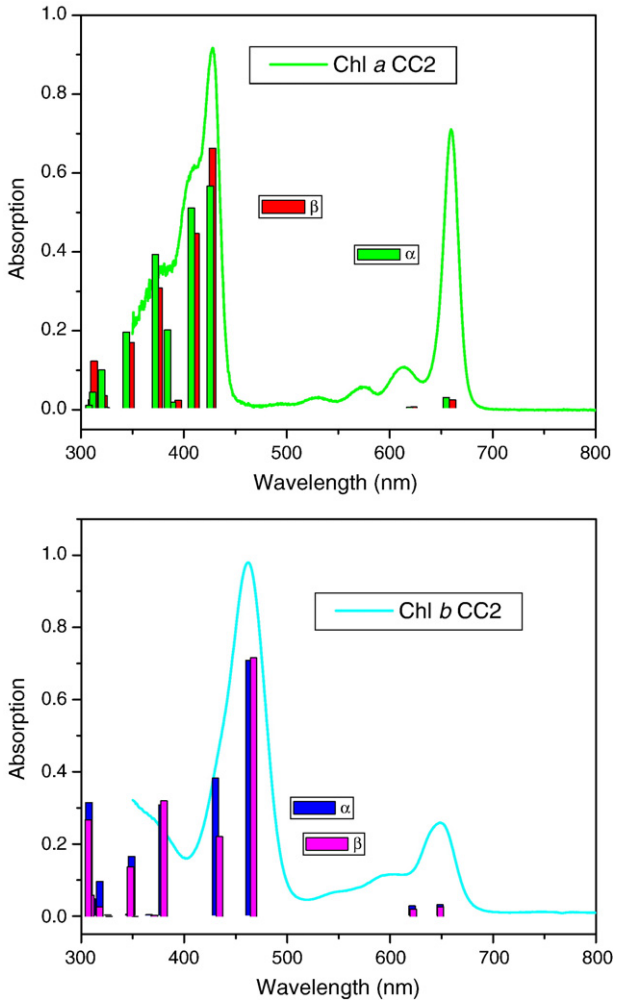


Fig. 3. Chl *a* and Chl *b* spectra [3] compared to the CC-RI *ab inito* calculations. The same arbitrary scaling factor was used to account for solvent effects for the α- and β-histidine ligated Chls. His ligated α-Chl *a*: green; His ligated β-Chl *a*: red; His ligated α-Chl *b*: blue; His ligated β-Chl *b*: magenta.

of the absorption wavelength by the protein matrix that is associated with slight variations of the torsion angle between this 3-vinyl group and the Chl mean plane.

Comparison of the data in Table 1 between the Chls and the dihydro-Chls for both *a* and *b* cases is informative. Larger band shifts are encountered when the 3-vinyl group interrupts its conjugation with the macrocycle than those which can be attributed to the α- or β-ligation of the magnesium atoms by the apoprotein. By analysing the vinyl torsion angle for the 96 Chls *a* in PSI and the 35 Chls *a* in PSII we find that actually very few Chls have a fully conjugated 3-vinyl group with a C2–C3–C3^1–C3^2 dihedral angle around 0° or 180° and that most favour a 60°/−120° orientation as shown in Fig. 4. We find that an almost fully conjugated 3-vinyl group (with a dihedral angle of ~28° at the DFT/B3LYP/TZVP level) leads to negligible bathochromic shifts of ~0.7 nm and ~1.4 nm for Chl *a* and Chl *b*, respectively. We assume that a 90° twisted 3-vinyl group has no orbital overlap with the macrocycle and is thus comparable to the 3-ethyl group of the dihydrochlorophylls. The 60°/−120° orientations, which are also the most common, increase only slightly the formation enthalpy calculated in vacuum but still show sufficient conjugation being slightly (~5 nm) more red-shifted in comparison with the dihydrochlorophylls. It appears thus, that the protein matrix can fine tune the absorption maxima of its Chls by slightly changing the orientation of the 3-vinyl group through pure steric interactions. Further important shifts can be induced by positioning charged amino acid residues close to the tetrapyrrole chromophores. These electrochromic shifts are difficult to estimate with comparable precision using quantum chemical methods. Recently, site energies which also consider the protein backbone, have been computed with a combined quantum chemical and electrostatic approach [50]. Finally, the largest perturbations which can be induced in the monomeric Chl absorption and emission wavelengths are through excitonic interactions between closely spaced chromophores [51]. Either Chl-carotenoid or Chl–Chl interactions within dimers or oligomers can shift by as much as 50 nm the absorption wavelength. Presently, calculations for a Chl dimer are beyond the scope of reliable quantum chemical *ab initio* methods. At a semiempirical level, such as ZINDO S [52], calculations have shown that for a stacked Chl *a* dimer, the monomer absorption can be shifted from 666 nm, which is encountered e.g. in dilute diethyl ether solution [3] to as much as 700 nm as encountered for the special pair P700 in PSI [31].

2.2. Functional relevance of the diastereotopic ligation of Chls

2.2.1. Comparison between PSI and PSII

Out of the 96 Chls in the PSI monomer only 14 are β-ligated, and these occupy preferential positions surrounding the RC [31]. Our previous attempts to distinguish clearly between α- and β-ligands based on earlier lower resolution PSII structures [9,10] in the absence of the electron density map, proved to be very uncertain. We have now analysed the ligands in PSII based on the very recent high resolution structure at 2.9 Å [13]. By using these newer electron density maps we are now confident on most of the α/β-assignments, and these are presented in Table 2.

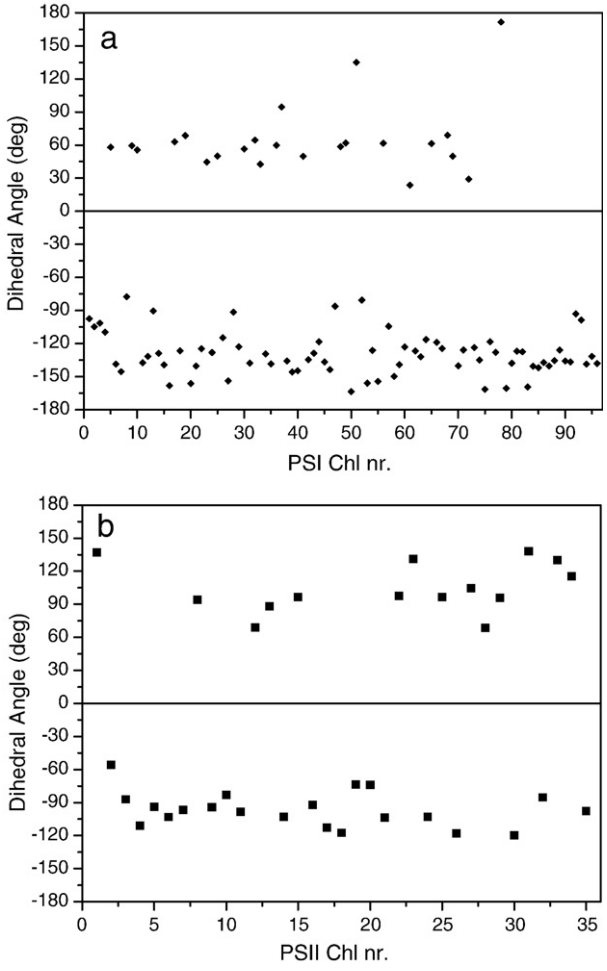


Fig. 4. Conformational distribution of the 3-vinyl group of Chl *a* in PSI (a) and PSII (b). The dihedral angle is defined by C2–C3–C3^1–C3^2.

Author's personal copy

Table 2
Chlorophylls and their ligands from the PSII structure at 2.9 Å resolution [13].

PDB Nr. 2AXT (3.0 Å)	PDB Nr. 3BZ1 (2.9 Å)	Ligand and distance to Mg	Phytyl chain position	Diastereotopicity	Equivalent Chl in PSI
1	A362	His A-198 NE2, 2.27 Å	Away from ring	α, P680	1011, α
2	D354	His D-197 NE2, 2.19 Å	Away from ring	α, P680	1021, α
3	A363	Thr A-179 OG1[a], 4.95 Å	Away from ring β blocked by Pheo5	α, acc. Chl	1012, α
4	D364	Gly D-174 O[a]?, 6.14 Å (α) Val D-175 O[a]?, 6.64 Å (α) Chl2 O2A[a]? 6.64 Å (β)	Away from ring β blocked by A-Phe206 and Pho355D	α?, acc. Chl	1022, α
7	A366	His A-118NE2, 2.44 Å	Away from ring	α	n.e.
8	D356	His D-117NE2, 2.55 Å	Away from ring	α	n.e.
11	B511	Trp B-185O[a]?, 4.19 Å	Phytol on side of ring, α-side towards membrane	β	n.e.
12	B512	His B-201ND1, 2.36 Å	Away from ring	α	1116, α
13	B513	His B-202NE2, 2.36 Å	Partly on β-side	α	1117, α
14	B514	His B-455NE2, 2.40 Å	Away from ring	α	1127, α
15	B515	His B-100NE2, 2.51 Å	Away from ring	α	n.e.
16	B516	His B-157ND1, 2.35 Å	Away from ring	α	1112, α
17	B517	Met B-37SD[a]?, 4.55 Å MGDG 533(O10)[a], 3.92 Å	Away from ring	α? β?	n.e.
21	B518	His B-466NE2, 2.37 Å	Curls under Mg	α	n.e.
22	B519	His B-216NE2, 2.36 Å	β blocked by Car H107	α	1119, α
23	B520	Ser B-240OG[a]?, 4.05 Å Ser B-241OG[a]?, 4.84 Å	α blocked by Chl B519	β?	1123, β
23	B520	Ser B-240OG[a]?, 4.05 Å Ser B-241OG[a]?, 4.84 Å	α blocked by Chl B519	β?	1123, β
24	B521	His B-469NE2, 2.37 Å	β blocked by Chl B523 phytyl	α	1128, α
25	B522	His B-23NE2, 2.75 Å	α blocked by Chl B521	β	1103, β
26	B523	His B-26NE2, 3.06 Å	Curls on α side, not tightly, α blocked by Chl B521 phytyl	β	1104, β
27	B524	His B-9NE2, 2.28 Å	Curls under Mg, blocks β	α	1102, α
28	B525	His B-142NE2, 3.05 Å	Phytyl curls over to α side, α side blocked by Chl B526	β	1111, β
29	B526	His B-114NE2, 2.88 Å	Curls to the other side, α blocked by Chl B525 phytyl	β	1108, α
33	C474	His C-237NE2, 2.23 Å	At side of ring, β blocked by phytyl of Chl C476	α	1215, α
34	C475	His C-430NE2, 2.41 Å	Away from ring, β blocked by phytyl of Chl C476C	α	1225, α
35	C476	His C-118NE2, 2.29 Å	20, curls under Mg not sharply, β blocked by phytoyl of Chl C475	α	n.e.
37	C477	DGDG 205 (AO1), 3.47 Å Met C-67SD[a], 4.55 Å	Away from ring	β? α?	n.e.
41	C478	His C-441NE2, 2.22 Å	Curls under Mg sharply	α	n.e.
42	C479	His C-251NE2, 2.34 Å	β blocked by phytyl of Chl C479 and C480	α	1216, α
43	C480	Ser C-275OG[a], 4.22 Å	Curls over to α side, not sharply, α blocked by ring of Chl C479	β	1221, β
44	C481	His C-444NE2, 2.34 Å	Curls under, not sharply, β blocked by phytyl of Chl C483	α	1226, α
45	C482	His C-53NE2, 2.84 Å	Curls back to β side of ring	β	1202, β
46	C483	His C-56NE2, 2.88 Å	Curls over under Mg	β	1203, β
47	C484	Asn C-39OD1, 2.24 Å	β blocked by Car C487	α	1231, α
48	C485	His C-164NE2, 2.95 Å	Phytyl away from ring, α blocked by Chl C486 and Car Z116	β	1210, β
49	C486	His C-132NE2, 2.23 Å	Curls under, not sharply	α	1208, α

n.e.: no equivalent.
[a] Possible indirect ligands.

Fig. 2 shows examples of α- and β-ligated Chls from the PSII 2.9 Å resolution crystal structure [13]. The uncertainty of the α- *versus* β-ligation was much larger at 3.5 Å resolution [10], and this precluded definite assignments and conclusions to be drawn, although attempts of educated guesses have been made [36,53].

Of the total of 35 Chl *a* in the 2.9 Å resolution structure of PSII we could identify 6 Chl bound to D1 and D2 subunits, 13 to CP43 and 16 to CP47. Of these 35 Chl a total of 22 are certainly ligated in the α-configuration, nine are found certainly as β-ligated and four are uncertain. For these remaining Chl the ligand to the central Mg^{2+} ion could not be identified unambiguously, although a qualified guess is possible for most of them. Assuming the most probable ligation, three of these four Chl (Chls B517, B520, C477) are β-ligated, whereas one (Chl D364) is most likely α-ligated. The numbering of Chls is as in the 2.9 Å structure [13] (PDB file 3BZ1, see also Table 2). Based on these assumptions a total of 24 Chls (~66%) are found as α- and eleven (~34%) as β-ligated. Interestingly, the distribution of ligands is different for both types of Chls, e.g. the percentage of non-His ligands for β-Chl is twice as high compared to α-Chl (42% compared to 13%). These non-His ligands include Ser, Trp, lipids (mono- and digalactosyldiglycerols, MGDG and DGDG) for β-Chl and Thr, Gly, Asn, for α-Chl (most of them as an indirect ligand). The arrangement of β-Chl follows the pseudo *C2*-symmetry relating D1CP43 with D2CP47 (pseudo-*C2*(Fe^{2+}), [11]). This is visible as the β-Chls are more or less equally present in CP43 (5) and CP47 (7), and all five β-Chls found in CP43 have a symmetry related counterpart in CP47. The only exception is β-Chl B526 (previously nr. 29 in ref. [11]) in CP47 whose counterpart in CP43 (Chl C486) is an α-Chl (see Fig. 5). Very recently, Raszewski and Renger have assigned this Chl B526 as the most red-shifted Chl in PSII [54], and when its ligand (His B114) was mutated to Tyr, the 695 nm emission band disappeared with concomitant loss of oxygen production [55]. The β-Chl B526 appears thus to be essential for full functionality of PSII. It is also in close proximity (4.8 Å shortest π–π distance) to a carotenoid (Car 6, BCR B530) which can thus quench the dangerous triplet state, should this be formed.

Astonishingly, the β-Chls are nearly exclusively located in the stromal layers in CP43 and CP47 with only β-Chls 11, 17 and 37 being located in the lumenal layers of the photosynthetic membrane [13] (see Fig. 5). This matches exactly the height of the stromal layer of the major plant LHC II containing also the 2 β-Chls *a* and the only β-Chl *b* [33].

Eight of the β-Chls in PSII have β-Chl counterparts in PSI, three have no equivalent Chl at the same position in PSI and only one β-Chl

Author's personal copy

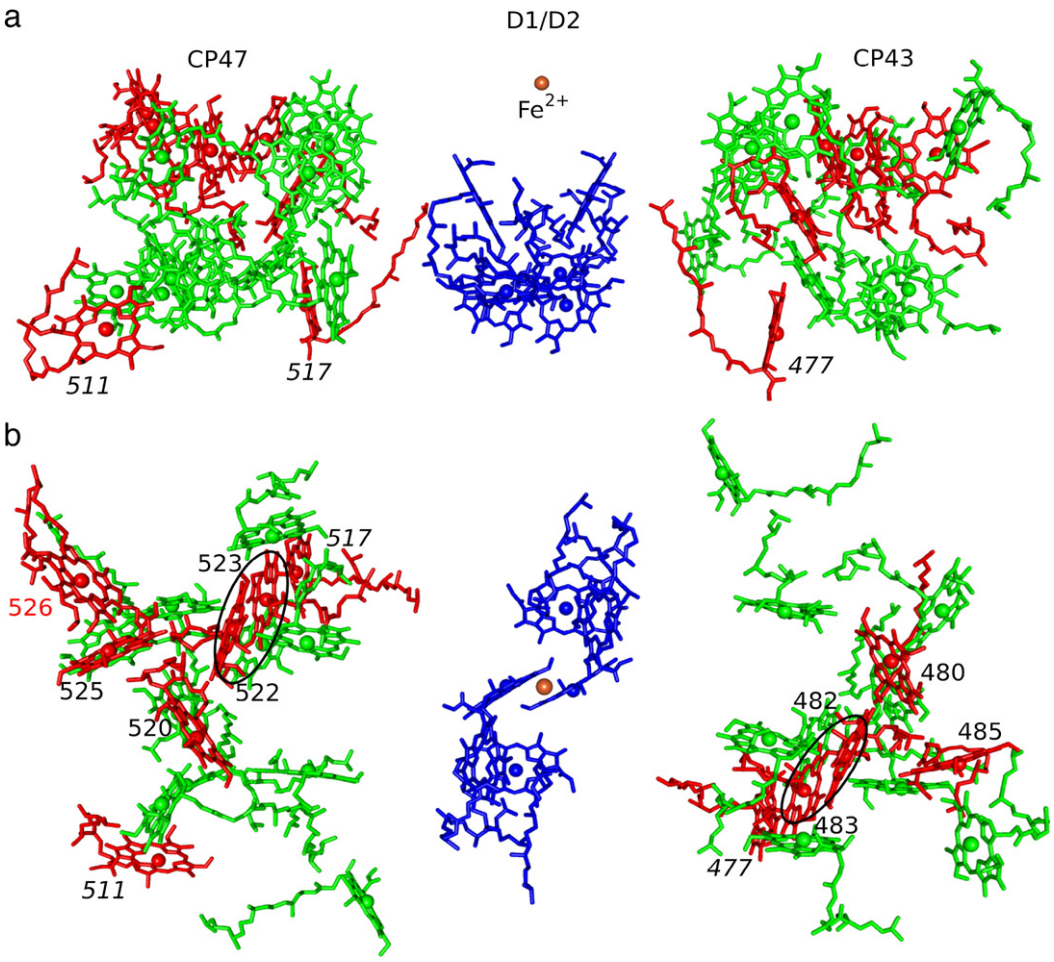


Fig. 5. Positions of β-Chls in PSII. a) Side view along the membrane plane with cytoplasm at top and lumen at bottom; b) top view onto the membrane plane from the cytoplasmic/stromal side. β-Chls are shown in red, α-Chls in green, RC-Chls and Phe (subunits D1/D2) in blue, the non heme Fe^{2+} as orange sphere. For Chls with uncertainty about the exact ligand, the most probable ligation as detailed in the text was assumed. The numbers for the β-Chls are given in italics for β-Chls located in the lumenal layer in both panels and in normal text for β-Chls located in the stromal layer (panel b) only). In addition, in panel b), the red-shifted β-Chl B526 is highlighted with a red label and the pairs of β-Chls in CP43 and CP47 are marked by black elipses. The image was generated with PyMol using pdb entry 3bz1.

(the special Chl B526) in PSII has an α-Chl in PSI at the conserved position. PSI has a total of 14 β-Chls, but only eight of these are found at positions conserved also in PSII, and all of these positions in PSII also contain a β-Chl. Since this cannot be due to random assembly, a very similar folding process of the apoproteins must occur which bind specifically the α- or β-Chls at predetermined positions.

In PSI, each PsbA and PsbB side harbours a dimer of β-Chls situated equidistantly at 31 Å from P700. The dimers are formed by Chl 1103 and Chl 1104 with a center-to-center distance of 9.5 Å and shortest *π*–*π* distance of 5.4 Å in PsaA and by Chl 1202 and Chl 1203 with a center-to-center distance of 9.3 Å, shortest *π*–*π* distance of 5.4 Å in PsaB. In both cases the ligands (PsaA His76, His79; PsaB His49, His52) are on the same helix. This results in an arrangement shown in Fig. 6 (top), where the two β-Chls with the α side of the first Chl (1103 or 1202) are facing the β side of the second Chl (1104 or 1203). Interestingly, a comparable arrangement is also found in PSII, Fig. 6 (bottom). In each CP43 and CP47, a dimer of β-Chls (Chls B522, B523 in CP47 and Chls C482, C483 in CP43) is encountered at nearly the same distance to Chl pair $P_{D1/D2}$ (33 Å). The observed distances (9.5 Å center-to-center and 5.4 Å *π*–*π* distance) are within the error limits similar to the values found in PSI, and also here the α side of one Chl faces the β side of the partner Chl. This arrangement makes only limited use of the advantage which a β-ligation would bring, compared to an α-ligation, with respect to the possibilities of dimer formation, as the β-β dimers put into evidence do not have their "free" α faces fully facing each other.

An interesting feature which seems to be strongly conserved is that such Chl dimers are ligated by histidines which are closely spaced within the same protein subunit. Thus as both ligands come from the same side, the free α side of one tetrapyrrole interacts strongly with the β side of the other dimer half. In all cases the 17-propionic acid residue of this second half curls back onto the other (α) side allowing for a more favourable *π*–*π* stacking interaction. Furthermore, as put into evidence by Fig. 7, because in PSII these traps have practically the same spatial distribution as the ones in PSI, this proves that there must have been a common ancestor in photosynthesis for engineering efficient light-trapping. We thus favour the hypothesis that electronic excitation energy transfer occurs from the peripheral antenna to the reaction center via preferential pathways which may involve these special β-ligated Chls for structural reasons. The protein folding leading to the assembly of PSI and PSII must take similar pathways as to incorporate β-ligated Chls at similar and conserved positions. The influence of the protein backbone can also be very different for the two diastereotopic ligations as was shown by a statistical analysis in PSI [37] and as we describe herein for PSII.

A β–β dimer model showing strong excitonic coupling in PSII is shown schematically in Fig. 6 (center in red). Raszewski and Renger have calculated the couplings (supporting information of reference [54]) between the Chls within CP43 and CP47. For the dimer formed by Chl C482 and Chl C483 of CP43 a value of $-50\ cm^{-1}$ was found. The three lowest site energies, that is the redmost pigments of CP43

Author's personal copy

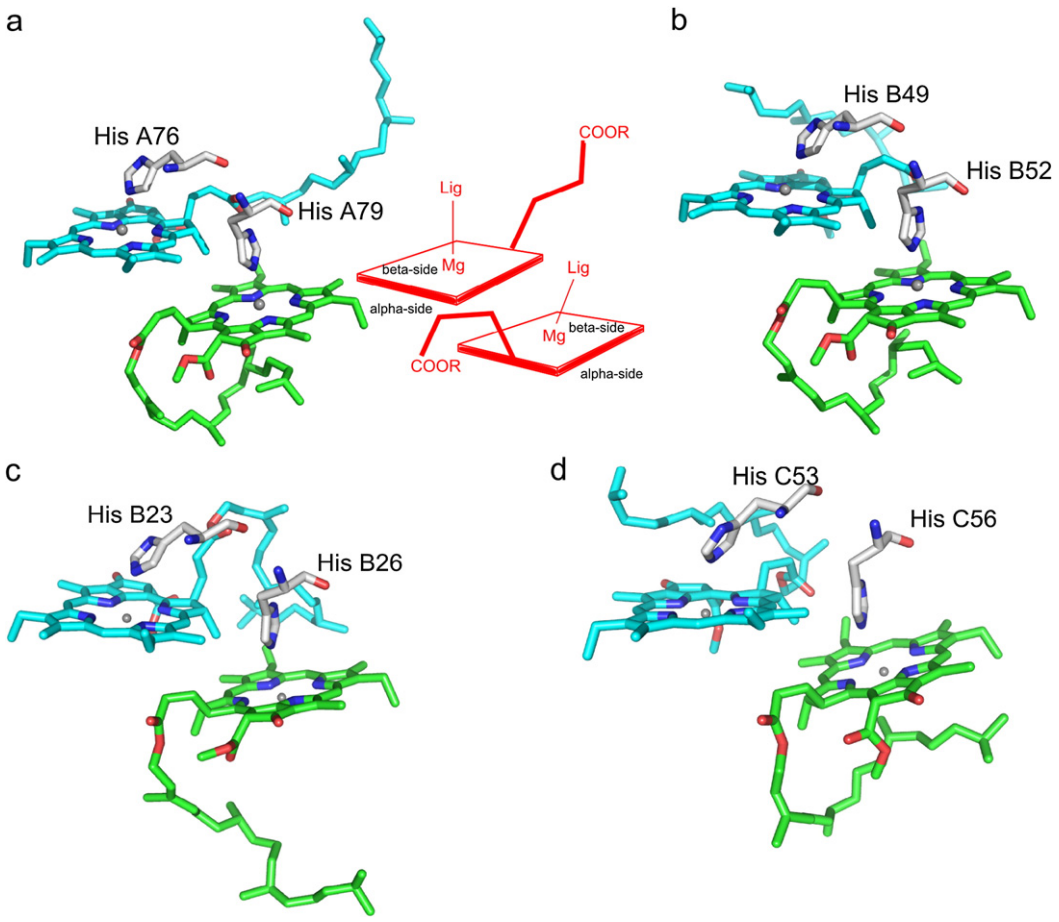


Fig. 6. The β,β-Chl dimers encountered in PSI and PSII. a) β,β-Chl dimer formed by Chl 1103 (carbons in cyan, ligated by His A76) and 1104 (carbons in green, ligated by His A79) in PsaA of PSI. Next to it the one (out of four possible) conformation that is found for all of the β,β-Chl dimers in PSI and PSII is shown schematically in red. b) β,β-Chl dimer formed by Chl 1202 (carbons in cyan, ligated by His B49) and 1203 (carbons in green, ligated by His B52) in PsaB of PSI. c) The β,β-Chl dimer formed by Chl B522 (in cyan) and Chl B523 (in green) and the ligating His (His B23 and His B26, light grey) from subunit CP47 (PsbB) in PSII. d) The β,β-Chl dimer formed by Chl C482 (in cyan, ligated by His C53) and Chl C483 (in green, ligated by His C56) found in subunit CP43 (PsbC) in PSII. The figure was generated using the program PyMol and PDB entries 3bz1 (PSII) and 1jbo (PSI).

were assigned to Chls 37, 43 and 45, all three being highly probably β-ligated. Thus the lowest energy exciton appears to be delocalised over one dimer half comprising Chl C482 and Chl C480. The coupling between Chl C482 and C480 was calculated to be 64 cm^{-1}. On the side of CP47, the β–β dimer formed from Chls B522 and B523 has a calculated coupling of −64 cm^{-1}. As mentioned above, the redmost pigment was assigned to Chl B526 which is quite far from the RC. The red Chl proximal to P680 was assigned as α-Chl B521 which has a calculated coupling of 52 cm^{-1} with the β-Chl B522. It is thus probable that the directionality of energy transfer can be switched from the trap formed by Chls B521, B522, and B523 towards P680, or in a dissipative mode, towards β-Chl B526. This could explain the energy dissipation when PSII is switched in a photoprotective mode. In order to test this hypothesis, in the future we suggest mutating the His ligands of the β-Chls B522 and B523 and studying both the primary and secondary electron transfer processes spectroscopically. Very recently, Tracewell and Brudvig have brought forth convincing evidence for Chls within CP43 and CP47 to be oxidized by $P680^{+}$ [56].

2.2.2. The B850 ring from purple bacteria LH2 is formed exclusively with β-BChls a

The light-harvesting complexes of purple photosynthetic bacteria are formed by self-assembly of small polypetides which bind BChl *a*. The smaller LH2 complex is circular and is formed by two concentric rings of BChls *a*, one absorbing at 800 nm (B800) and a more red-shifted ring absorbing at 850 nm (B850). The larger LH1 complex is elliptical and contains the reaction center (RC).

The B850 ring of *Rhodopseudomonas acidophila* [16,18] or *Rhodospirillum molischianum* [17] are formed exclusively by 18 or 16 β-BChls *a*, respectively. However, histidines situated on different polypeptides now ligate the interacting macrocycles from opposite positions so that strong excitonic interactions occur both between two α and two β sides as shown in Fig. 8. Dimers with alternating α,α- and β,β-interactions are thus formed. The two free α-sides are somewhat closer having a Mg–Mg distance of 9.15 Å than the two β-sides which confer a 9.44 Å distance between the Mg atoms. One cannot strictly speak in this case of "special" β–β dimers as the exciton is delocalized over the whole B850 ring which thus has a red-shifted absorption by 50 nm in comparison to isolated BChl *a* molecules forming the B800 ring. The β ligation provides thus a structural explanation for the observed red shift which arises from strong excitonic coupling rather than modified site energies.

From the present LH1 crystal structure [14] it is not possible to clearly discern whether the 30 BChls *a* are β-ligated or not. If this should be the case, it would explain an efficient energy transfer relay to the engulfed RC by structurally matching the peripheral LH2 B850 β-Chls.

2.2.3. The minor antenna complex CP29 contains an α–β-Chl heterodimer

In the minor antenna complex CP 29, the A5–B5 pair of chlorophylls was very recently shown to be involved in a charge-

Author's personal copy

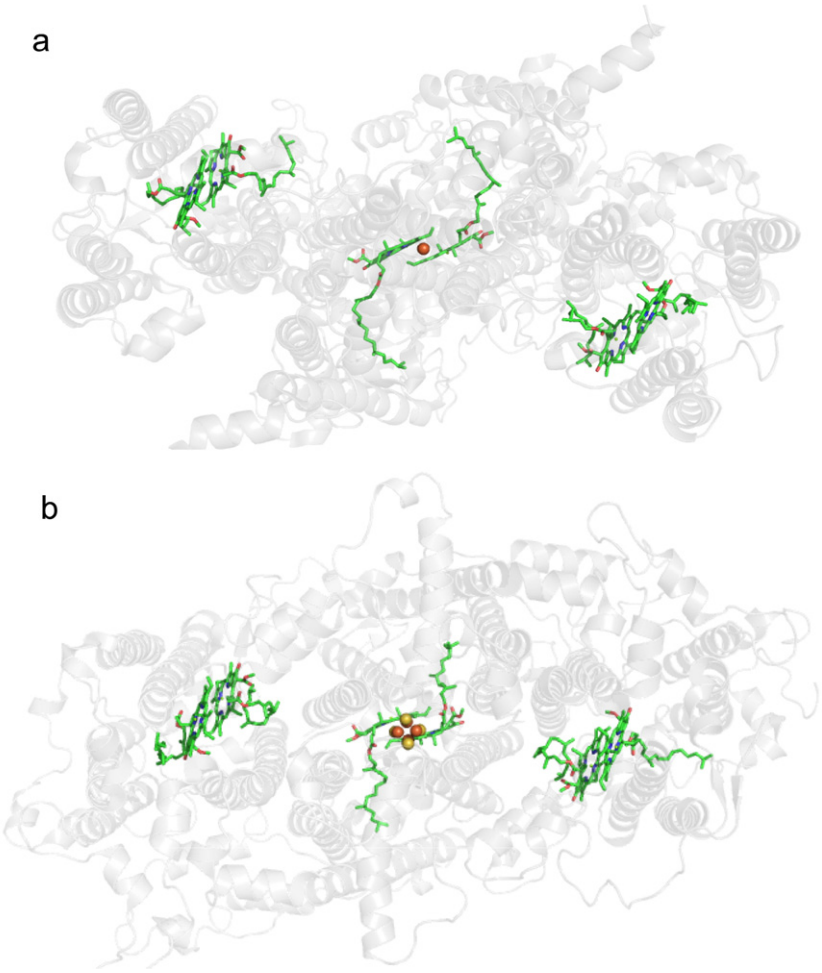


Fig. 7. Comparison of the position of the β,β-Chl dimers in PSII and PSI. a) Location of the two pairs of β-Chl, composed of Chl B522 and B523 in CP47 and Chl C482 and C483 in CP43 in relation to the non hem Fe^{2+} (orange sphere) and the central Chl pair P_{D1}/P_{D2} of PSII. The subunits D1, D2, CP43 and CP47 are shown in light grey in cartoon mode. b) Location of the two pairs of β-Chl, composed of Chl 1103 and 1104 in PsaA and Chl 1202 and 1203 in PsaB in relation to the Fe_4S_4 cluster F_X (orange and yellow spheres) and the central pair of Chl 1011 and 1021 in PSI. The subunits PsaA and PsaB are shown in light grey in cartoon mode, distances are given in Å.

transfer state with a nearby situated zeaxanthin regulating thus light-harvesting by nonphotochemical quenching [57]. In Fig. 9 the two related Chls from the structure of the LHCII complex [28] are shown. Assuming a high structural homology between CP29 with an unknown X-ray structure, and LHCII, one can clearly distinguish the same type of dimer involving a β-Chl having the phytyl chain curling back on the α-side leaving a relatively free β-side which now interacts favourably with an α-Chl.

2.3. Statistical analysis of Chl-binding pockets in photosystem II

To further understand the differences between Chl ligated in the α- or β-configuration, and thus investigate the role of the distinct ligations, we turned our attention to the interactions between α- and β-ligated Chls with the apoprotein. As a detailed study on the 96 PSI Chls has been recently published [37], we concentrate here on the analysis of the new PSII crystal structure.

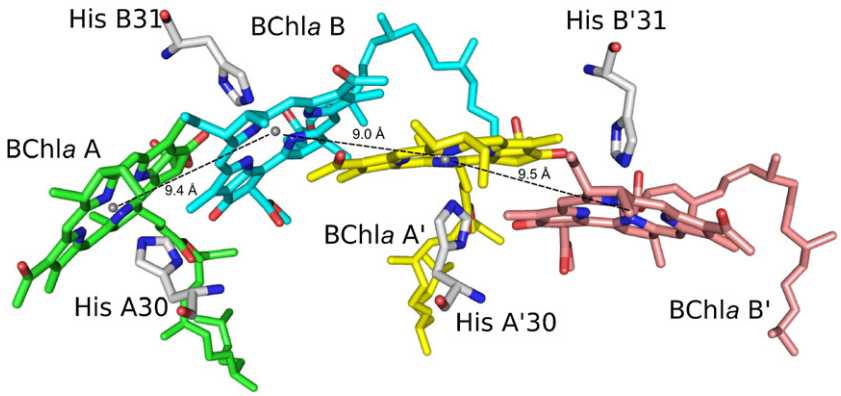


Fig. 8. Four BChls *a* of the B850 ring in LH2 of *Rhodopseudomonas acidophila* [18] (pdb code 1nkz). The two BChls *a* A and A' (carbons in green and yellow, respectively) are coordinated by two copies of subunit A, the two BChls *a* B and B' (carbons in cyan and salmon, respectively) are coordinated by two copies of subunit B. Note the clear β-ligation of all four BChls *a* by histidines 30 and 31 (carbons in grey), respectively. The distances between the four central Mg atoms are given in Å. The figure was generated using PyMol.

Author's personal copy

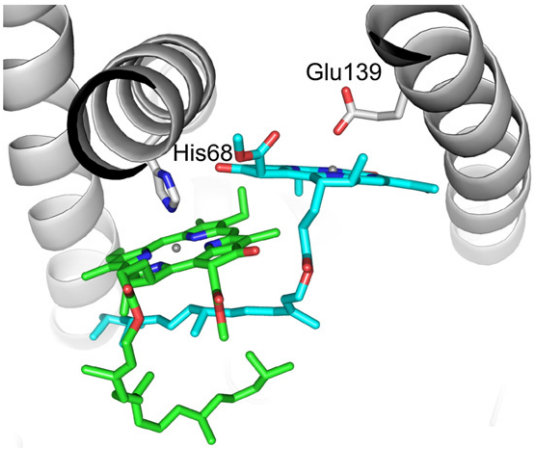


Fig. 9. An α–β-Chl dimer in LHCII as found in the 2.5 Å resolution structure from pea [28] as a model for the spectroscopically characterised Chl dimer in the minor antenna protein CP29 [57]. Shown are the β-Chl *a* (carbons in green, nitrogen in blue, oxygen in red) ligated by His 68 (carbons in light grey) and the α-Chl *b* (carbons in cyan) ligated by Glu 139. Assuming a high structural homology between LHCII and the minor antenna protein CP29 the Chl dimer A5–B5 in CP29 is expected to have a similar arrangement as the equivalent α–β-Chl dimer in LHCII shown here. The figure was generated using the PDB entry 2bhw and the program PyMol.

PSII binds a total of 35 Chl per monomer, of which probably a maximum of twelve are bound in the "β-position" (*vide supra* Table 2 and Fig. 5). It thus constitutes a considerable data base for Chl-binding studies, in particular, for statistical analyses of the Chl-binding pockets. The protein environments have been analysed around the α- and β-ligated Chls of PSII (Fig. 10 a, b, c, d) within a radius of ≤5 Å. At first sight, the pattern of interacting atoms of PSII polypeptides and the α- and β-ligated Chl functional groups appear to be similar (Fig. 10 a, b). Contacts occur most frequently with the long substituents of the Chl macrocycle, in particular of rings B, C, and E. For α-ligated Chls, the $C13^4$ methoxy, the 13^3 C=O groups and the methyl groups of C12 and C18 have the highest number of contacts with the apoprotein(s). For β-ligated Chls, the $C13^1$ C=O group is conspicuously frequently in contact with the apoprotein in addition to the contacts delineated above. Relatively infrequent are contacts with the substituents of ring D and the atoms which make up the tetrapyrrole rings and methine bridges (see formula in Fig. 1). The amino acids taking part in these contacts are also similar for the two diastereotopic ligation forms. Naturally, histidine is frequently close to the nitrogen atoms which bind the central Mg atoms. Notably, the aromatic phenyalanine is often found to be close to Chls, in particular, around atoms that have little contact to histidines. Next to these two residues, the aliphatic residues leucine, isoleucine, valine as well as alanine and the aromatic residues tyrosine and tryptophan make up most of the residues in the Chl-binding pockets. Notably, Tyr and Trp are frequently found at ring C, in particular of β-ligated Chl. Polar and charged residues are present to a lesser degree but are equally distributed. Clear differences in the amino acid distributions between the two forms are observed for the $C13^3$ and $C13^4$ keto carbonyl and methoxy groups. These groups from α-ligated forms are frequently close to the basic residues Arg and Lys (Fig. 10 a, b).

Interestingly, the Chl-protein contacts vary significantly depending upon the α/β-Chl-ligation state when analyzed for the contacts with the binding helices. Fig. 10 c and 10 d show the contact maps for α- and β-ligated Chl with their respective binding helices, *i.e.* the helices which carry the ligating residue to the Chls' central Mg atom. These contact maps are clearly distinct for the two diastereotopic forms. The main differences are observed at rings E and the substituents at C13. In case of the β-ligated Chls (Fig. 10 d), there exist very few close contacts between residues of the α-helices and the atoms of ring E of Chl *a*. Remarkably, the keto carbonyl and methoxy groups of $C13^3$ and $C13^4$ of the β-ligated Chls are hardly ever found in the vicinity of a residue of the binding α-helices as observed previously in PSI [37] (Fig. 10 d). In contrast, the atoms of ring E of the α-ligated Chls are very frequently found in close vicinity of these residues (Fig. 10 d). Both, the $C13^1$ and $C13^3$ oxo as well as $C13^4$ of the α-ligated Chl are frequently in close contact with residues of the binding α-helices. Additional differences in the Chl-binding sites are observed for the atoms of ring D. In the case of the α-ligated Chls, contacts are conspicuously low (Fig. 10 c). For β-ligated Chls, however, the 18^1 methyl group is often found close to apoprotein.

This analysis indicates that significant differences exist between the binding pockets of the Chls, depending upon the ligation state. Due to the Chl conformation, the C13 substituents of an α-ligated Chl are facing the binding α-helix, and thus, they are usually in close contact with residues of these trans-membrane helices. The C13 substituents of β-ligated Chls, however, face to the opposite side and are less likely to be in close contact with the residues of the binding helices. In spite of this, there are a substantial number of contacts between the C13 substituents of the Chls ligated in the β-position and the protein environment (Fig. 10 b). As shown previously, the C-13 oxo

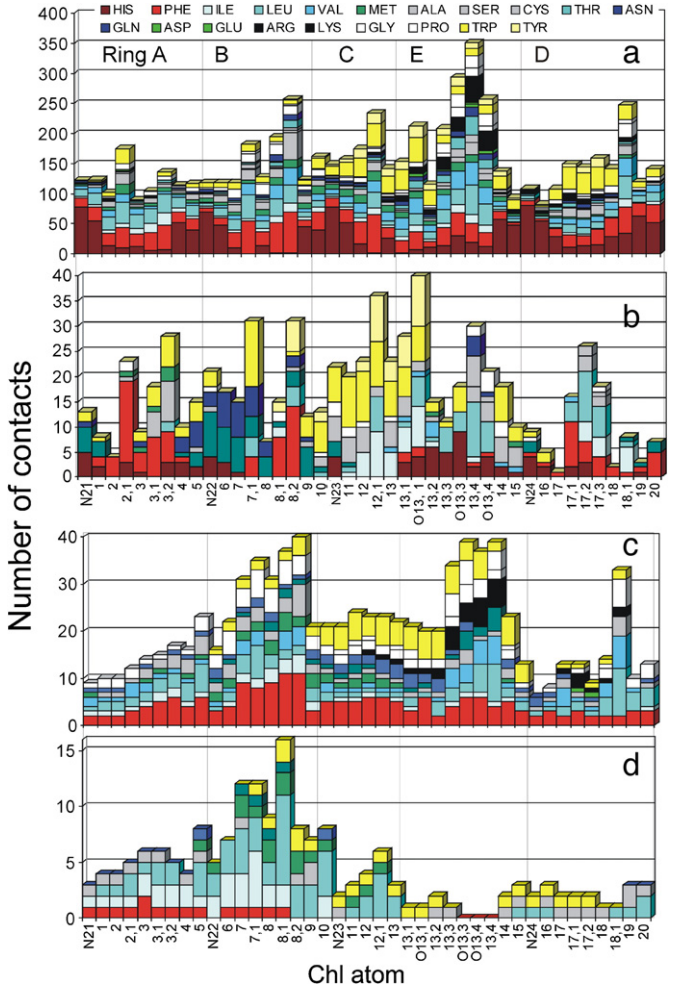


Fig. 10. Analysis of the α- and β-ligated chlorophyll polypeptide binding pockets in PSII. Contacts to the proteinaceous environment within a radius of ≤5 Å are shown for α-ligated Chls (a, c) and β-ligated Chls (b, d). Contacts between residues of the binding helices and the Chl atoms only (as compared to a and b in which contacts to the entire proteins are listed) are shown for α-ligated Chls (c) and β-ligated Chls (d). The binding helices are defined as the helices which provide the ligand for the central Mg atom. Each amino acid counts once no matter how many atoms are within ≤5 Å. The numbering of the Chl atoms is as in Fig. 1 and each atom has its own position numbered along the abscissa. Note, that in c and d, the contacts to the His ligands have been omitted for clarity. In addition, only Chls have been included in this analysis which are unambiguously identified as β- or α-ligated. The colour coding is as indicated in the legend.

Author's personal copy

of the Chls ligated in the β-position are chiefly engaged in H-bonds, in particular with helices other than the one ligating the central Mg [37]. It appears thus that the C = O groups of β-ligated Chls are engaged in interactions between adjacent α-helices. This may point either at their critical contribution to the overall assembly of the photosystem or alternatively, at the necessity to firmly anchor the β-Chl at distinct positions among the helices required for their role in the special energy transfer pathway.

3. Conclusions

Our study shows a remarkable similarity between the "special" β–β dimers encountered in PSI and PSII which points to a common ancestor and a similar mechanism for light-trapping from the peripheral antenna to the RC. The B850 ring in LH2 and probably also in the LH1 of purple bacteria are formed exclusively from β-ligated BChl *a*. In CP29 an α–β-heterodimer is implied in regulating light-harvesting. We conclude that the excitation energy transfer in light-harvesting systems from a peripheral antenna towards the reaction center can follow preferential pathways due to structural reasons, such as those engineered with "special" β-ligated (B)Chls. Definite proof of this conjecture could be obtained by spectroscopic studies combined with mutagenesis studies using for instance double mutants with the noninnocent β-ligands replaced by non-coordinating ligands for magnesium by knocking out selectively "special" β-ligated Chls in various chlorophyll–protein complexes.

Acknowledgements

STB is a founding member of the Center for Functional Nanostructures at the University of Karlsruhe and acknowledges partial financial support from the German Research Foundation (DFG) for project C3.5 "Energy Transfer Studies of Artificial Mimics of Natural Light Harvesting Molecules". JK, WS and AZ acknowledge support by the DFG in the frame of SFB 498 through projects A3 and C7. We thank Dr. Frank Müh for helpful suggestions.

References

[1] R.E. Blankenship, Molecular Mechanisms of Photosynthesis, Blackwell, Oxford, 2002.
[2] T.S. Balaban, Light-harvesting nanostructures, in: H.S. Nalwa (Ed.), Encyclopedia of Nanoscience and Nanotechnology, Vol. 4, American Scientific Publishers, Los Angeles, 2004, pp. 505–559.
[3] T.S. Balaban, H. Tamiaki, A.R. Holzwarth, Chlorins programmed for self-assembly in: F. Würthner (Ed.), Topics Curr. Chem., Supramolecular Dye Chemistry, 258, Springer Verlag: Heidelberg, 2005, pp. 1–38.
[4] R. van Grondelle, J.P. Dekker, T. Gillbro, V. Sundstrom, Energy transfer and trapping in photosynthesis, Biochim. Biophys. Acta 1187 (1994) 1–65.
[5] J. Deisenhofer, O. Epp, K. Miki, R. Huber, H. Michel, Structure of the protein subunits in the photosynthetic reaction centre of *Rhodopseudomonas viridis* at 3 Å resolution, Nature 318 (1985) 618–624.
[6] P. Jordan, P. Fromme, H.-T. Witt, O. Klukas, W. Saenger, N. Krauss, Three-dimensional structure of cyanobacterial photosystem I at 2.5 Å resolution, Nature 411 (2001) 909–917.
[7] M. Byrdin, P. Jordan, N. Krauss, P. Fromme, D. Stehlik, E. Schlodder, Light harvesting in photosystem I: modeling based on the 2.5 Å structure of photosystem I from *Synechococcus elongatus*, Biophys. J. 83 (2002) 433–457.
[8] A. Ben-Shem, F. Frolow, N. Nelson, Crystal structure of plant photosystem I, Nature 426 (2003) 630–635.
[9] A. Zouni, H.-T. Witt, J. Kern, P. Fromme, N. Krauss, W. Saenger, P. Orth, Crystal structure of photosystem II from *Synechococcus elongatus* at 3.8 Å resolution, Nature 409 (2001) 739–743.
[10] K.N. Fereira, T.M. Iverson, K. Maghlaoui, J. Barber, S. Iwata, Architecture of the photosynthetic oxygen-evolving center, Science 303 (2004) 1831–1838.
[11] B. Loll, J. Kern, W. Saenger, A. Zouni, J. Biesiadka, Towards complete cofactor arrangement in the 3.0 Å resolution structure of photosystem II, Nature 438 (2005) 1040–1044.
[12] B. Loll, J. Kern, A. Zouni, W. Saenger, J. Biesiadka, K.-D. Irrgang, The antenna system of photosystem II from *Thermosynechococus elongatus* at 3.2 Å resolution, Photosynth. Res. 86 (2005) 175–184.
[13] A. Guskov, J. Kern, A. Gabdulkhakov, M. Broser, A. Zouni, W. Saenger, Cyanobacterial photosystem II at 2.9 Å resolution: role of quinones, lipids, channels and chloride, Nat. Struct. Mol. Biol. 16 (2009) 334–342.
[14] A.W. Roszak, T.D. Howard, J. Southwall, A.T. Gardiner, C.J. Law, N.W. Isaacs, R.J. Cogdell, Crystal structure of the RC–LH 1 core complex from *Rhodopseudomonas palustris*, Science 302 (2003) 1969–1972.
[15] S. Bahatyrova, R.N. Frese, C.A. Siebert, J.D. Olsen, K. van der Werf, R. van Grondelle, R.A. Niederman, P.A. Bullough, C. Otto, C.N. Hunter, The native architecture of a photosynthetic membrane, Nature 430 (2004) 1058–1062.
[16] G. McDermott, S.M. Prince, A.A. Freer, A.M. Hawthornthwaite-Lawless, M.Z. Papiz, R.J. Cogdell, N.W. Isaacs, Crystal structure of an integral membrane light-harvesting complex from photosynthetic bacteria, Nature 374 (1995) 517–521.
[17] J. Koepke, X. Hu, C. Muencke, K. Schulten, H. Michel, The crystal structure of the light-harvesting complex II (B800–850) from *Rhodospirillum molischianum*, Structure 4 (1996) 581–597.
[18] M.Z. Papiz, S.M. Prince, T. Howard, R.J. Cogdell, N.W. Isaacs, The structure and thermal motion of the B800–850 LH2 complex from *Rps. acidophila* at 2.0 Å resolution and 100K: new structural features and functionally relevant motions, J. Mol. Biol. 326 (2003) 1523–1538.
[19] K.-H Zhao, P. Su, J-M. Tu, X. Wang, H. Liu, M. Plöscher, L. Eichacker, B. Yang, M. Zhou, H. Scheer, Phycobilin:cystein 84 biliprotein lyase, a near-universal lyase for cystein-84-binding sites in cyanobacterial phycobiliproteins, Proc. Natl. Acad. Sci. U. S. A. 104 (2007) 14300–14305 and further references therein.
[20] T.S. Balaban, A.R. Holzwarth, K. Schaffner, G.-J. Boender, H.J.M. de Groot, CP-MAS ^{13}C-NMR dipolar correlation spectroscopy of ^{13}C-enriched chlorosomes and isolated bacteriochlorophyll-*c* aggregates of *Chlorobium tepidum*: the self-organization of pigments is the main structural feature of chlorosomes, Biochemistry 34 (1995) 15259–15266.
[21] B.-J. van Rossum, D.B. Stensgaard, F.M. Mulder, G.-J. Boender, K. Schaffner, A.R. Holzwarth, H.J.M. de Groot, A refined model of the chlorosomal antennae of the green bacterium *Chorobium tepidum* from proton chemical shift constraints obtained with high-field 2-D and 3-D MAS NMR dipolar correlation spectroscopy, Biochemistry 40 (2001) 1587–1595.
[22] J. Pšenčik, T.P. Ikonen, P. Laurinmäki, M.C. Merckel, S.J. Butcher, R.E. Serimaa, R. Tuma, Lamellar organization of pigments in chlorosomes, the light harvesting complexes of green photosynthetic bacteria, Biophys. J. 87 (2004) 1165–1172.
[23] T.S. Balaban, Tailoring porphyrins and chlorins for self-assembly in biomimetic artificial antenna systems, Acc. Chem. Res. 38 (2005) 612–623.
[24] T. Jochum, C.M. Reddy, A. Eichhöfer, G. Buth, J. Szmytkowski, H. Kalt, D. Moss, T.S. Balaban, The supramolecular organization of self-assembling chlorosomal bacteriochlorophyll *c*, *d*, or *e* mimics, Proc. Natl. Acad. Sci. U. S. A. 105 (2008) 12736–12741.
[25] Y. Kakitani, Y. Koyama, Y. Shimoikeda, T. Nakai, H. Utsumi, T. Shimizu, H. Nagae, Stacking of bacteriochlorophyll *c* macrocycles in chlorosome from *Chlorobium limicola* as revealed by intermolecular ^{13}C magnetic-dipole correlation, X-ray diffraction, and quadrupole coupling in ^{25}Mg NMR, Biochemistry 48 (2009) 74–86.
[26] W. Kühlbrandt, D.N. Wang, Y. Fujiyoshi, Atomic model of plant light-harvesting complex by electron crystallography, Nature 367 (1994) 614–621.
[27] Z. Liu, H. Yan, K. Wang, J. Kuang, L. Gui, X. An, W. Chang, Crystal structure of spinach major light-harvesting complex at 2.72 Å resolution, Nature 428 (2004) 287–292.
[28] J. Standfu, A.C. Terwisscha van Scheltinga, M. Lamborghini, W. Kühlbrandt, Mechanisms of photoprotection and nonphotochemical quenching in pea light-harvesting complex at 2.5 Å resolution, EMBO J. 24 (2005) 919–928.
[29] D. Stroebel, Y. Choquet, J.-L. Popot, D. Picot, An atypical haem in the cytochrome b_{6f} complex, Nature 426 (2003) 413–418.
[30] G. Kurisu, H. Zhang, J.L. Smith, W.A. Cramer, Structure of the cytochrome b_6f complex of oxygenic photosynthesis: tuning the cavity, Science 392 (2003) 1009–1014.
[31] T.S. Balaban, P. Fromme, A.R. Holzwarth, N. Krauβ, V.I. Prokhorenko, Relevance of the diastereotopic ligation of magnesium atoms in chlorophylls in Photosystem I, Biochim. Biophys. Acta (Bioenergetics) 1556 (2002) 197–207.
[32] T.S. Balaban, Are *syn*-ligated (bacterio)chlorophyll dimers energetic traps in light-harvesting systems? FEBS Lett. 545 (2003) 97–102 Erratum FEBS Lett. 547 (2003) 235.
[33] T.S. Balaban, Relevance of the diastereotopic ligation of magnesium atoms of chlorophylls in the major light-harvesting complex II (LHC II) of higher plants, Photosynth. Res. 86 (2005) 251–262.
[34] T. Oba, H. Tamiaki, Coordination chemistry of chlorophylls: which side of the chlorin macrocycle is favored for the ligand coordination? J. Photosci. 9 (2002) 362–363.
[35] T. Oba, H. Tamiaki, Which side of the π-macrocycle plane of (bacterio)chlorophylls is favored for binding of the fifth ligand? Photosynth. Res. 74 (2002) 1–10.
[36] T. Oba, H. Tamiaki, Effects of peripheral substituents on diastereoselectivity of the fifth ligand-binding to chlorophylls, and nomenclature of the asymmetric axial coordination sites, Bioorg. Med. Chem. 13 (2005) 5733–5739.
[37] A. Garcia-Martin, L.G. Kwa, B. Strohmann, B. Robert, A.R. Holzwarth, P. Braun, Structural role of bacteriochlorophyll ligated in the energetically unfavourable β-position in light harvesting complex, J. Biol. Chem. 281 (2006) 1062610634.
[38] O. Christiansen, H. Koch, P. Jørgensen, The second-order approximate coupled cluster singles and doubles model CC2, Chem. Phys. Lett. 243 (1995) 409–418.
[39] M. Head-Gordon, R.J. Rico, M. Omu, T.J. Lee, A doubles correction to excited states from configuration-interaction in the space of single substitutions, Chem. Phys. Lett. 219 (1994) 21–29.
[40] C. Hättig, F. Weigend, CC2 excitation energy calculations on large molecules using the resolution of the identity approximation, J. Chem. Phys. 113 (2000) 5154–5161.
[41] C. Hättig, A. Hellweg, A. Köhn, Distributed memory parallel implementation of energies and gradients for second-order Møller-Plesset perturbation theory with

Author's personal copy

the resolution-of-the-identity approximation, Phys. Chem. Chem. Phys. 8 (2006) 1159–1169.
[42] R. Ahlrichs, M. Bär, M. Häser, H. Horn, C. Kömel, Electronic structure calculations on workstation computers: the program system Turbomole, Chem. Phys. Lett. 162 (1989) 164–169.
[43] F. Weigend, A. Köhn, C. Hättig, Efficient use of the correlation consistent basis sets in resolution of the identity MP2 calculations, J. Chem. Phys. 116 (2002) 3175–3183.
[44] D. Sundholm, Density functional theory calculations of the visible spectrum of chorophyll *a*, Chem. Phys. Lett. (1999) 480–484.
[45] T. Pullerits, V. Sundstrom, Photosynthetic light-harvesting pigment–protein complexes: toward understanding how and why, Acc. Chem. Res. 29 (1996) 381–389.
[46] Z.-L. Cai, M.J. Crossley, J.R. Reimers, R. Kobayashi, R.D. Amos, Density functional theory for charge transfer: the nature of the N-Bands of porphyrins and chlorophylls revealed through CAM-B3LYP, CASPT2, and SAC-CI calculations, J. Phys. Chem. B 110 (2006) 15623–15624.
[47] T.S. Balaban, High-five for magnesium complex, Chemical & Engineering News (ACS) May 16 (2005) 6.
[48] J. Heimdal, K.P. Jensen, A. Devarajan, U. Ryde, The role of axial ligands for the structure and function of chlorophylls, J. Biol. Inorg. Chem. 12 (2007) 49–61.
[49] J.K. Hoober, L.L. Eggink, M. Chen, Chlorophylls, ligands and assembly of light-harvesting complexes in chloroplasts, Photosynth. Res. 94 (2007) 387–400.
[50] F. Müh, M. El-Amine Madjet, J. Adolphs, A. Abdurahman, B. Rabenstein, H. Ishikita, E.-W. Knapp, T. Renger, α-Helices direct excitation energy flow in the Fenna–Matthews–Olson protein, Proc. Natl. Acad. Sci. U. S. A. 104 (2007) 16862–16867.
[51] M. Kasha, H.R. Rawls, M. Ashraf El-Bayaoumi, The exciton model in molecular spectroscopy, Pure Appl. Chem. 11 (1965) 371–392.
[52] HyperChem 7.01 Programme Package, HyperCube Inc., Gainesville, Florida 32601, USA.
[53] J.W. Murray, J. Duncan, J. Barber, CP43-like chlorophyll binding proteins: structural and evolutionary implications, Trends Plant Sci. 11 (2006) 152–157.
[54] G. Raszewski, T. Renger, Light harvesting in photosystem II core complexes is limited by the transfer to the trap: can the core complex turn into a photoprotective mode? J. Am. Chem. Soc. 130 (2008) 4431–4446.
[55] G. Shen, W.F.J. Vermaas, Mutation of chlorophyll ligands in the chlorophyll-binding CP47 protein as studied in a *Synechocystis* sp. PCC 6803 photosystem I-less background, Biochemistry 33 (1994) 7379–7388.
[56] C.A. Tracewell, G.W. Brudvig, Multiple redox-active chlorophylls in the secondary electron-transfer pathways of oxygen-evolving photosystem II, Biochemistry 47 (2008) 11559–11572.
[57] T. Kyu Ahn, T.J. Avenson, M. Ballottari, Y.-C. Cheng, K.K. Niyogi, R. Bassi, G.R. Fleming, Architecture of a charge-transfer state regulating light harvesting in a plant antenna protein, Science 320 (2008) 794–797.